

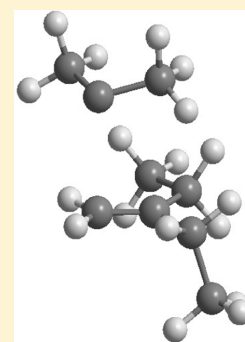
Nucleophilic Intermolecular Chemistry and Reactivity of Dimethylcarbene

Hui Cang, Robert A. Moss,* and Karsten Krogh-Jespersen*

Department of Chemistry & Chemical Biology, Rutgers, The State University of New Jersey, New Brunswick, New Jersey 08903, United States

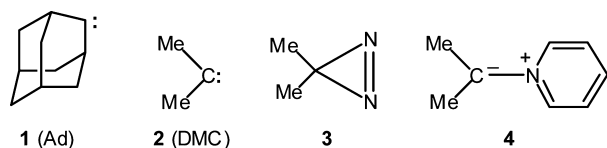
S Supporting Information

ABSTRACT: Experimental and computational studies find that dimethylcarbene (DMC), the parent dialkylcarbene, is both predicted to be and functions as a very reactive nucleophilic carbene in addition reactions with five simple alkenes. Activation energies and enthalpies for DMC additions to 2-ethyl-1-butene and methyl acrylate are computed and observed to be negative.



INTRODUCTION

We recently reported that the structurally constrained dialkylcarbene adamantanylidene (**1**, Ad) expresses both high reactivity and nucleophilic selectivity in its addition reactions with simple alkenes¹ and styrene derivatives.² Theoretical and computational considerations paralleled the experimental findings.¹ Our interest has now turned to dimethylcarbene (**2**, DMC), the parent dialkylcarbene. Will it too display nucleophilic intermolecular chemistry?



Experimentally assessing the intermolecular proclivities of DMC, however, is a much more difficult task than the analogous study of Ad. The *intramolecular* chemistry of Ad is modulated by its tricyclic structure, where the otherwise normative 1,2-hydride shift of alkylcarbenes here leads to an anti-Bredt alkene and is suppressed in favor of a relatively “slow” 1,3-CH insertion (with rate constant $k \sim (1-5) \times 10^7 \text{ s}^{-1}$ in isooctane or cyclohexane).^{3,4} As a result, Ad exhibits a robust intermolecular chemistry, adding in good yields to a variety of alkenes.^{5,6} The situation is quite different with DMC, as described in Platz’s classic report.⁷ Not only does the unconstrained parent dialkylcarbene undergo a rapid 1,2-H shift to propene ($k \sim 5 \times 10^7$ to $1.5 \times 10^8 \text{ s}^{-1}$ in various solvents,⁸ with an activation energy of $\sim 2.6 \text{ kcal/mol}$ in perfluorohexane⁷), but this rearrangement is accompanied by a significant quantum mechanical tunneling component. Additionally, some propene product may arise directly via

rearrangement and nitrogen loss from a photoexcited state of the carbene’s dimethyldiazirine (**3**) precursor, or from excited singlet DMC.⁷⁻¹⁰ Noncarbenic loss of its precursor would, of course, diminish the potential for intermolecular chemistry of DMC. Nevertheless, in an expression of *electrophilic* intermolecular chemistry, DMC can be trapped by pyridine to give ylide **4**.^{7,11}

The two key questions that we consider in the present report are as follows: (1) Can DMC be trapped by alkenes? (2) If it can be trapped, what kind of philicity does it display? Our responses to these queries constitute the first extended description of the *intermolecular* chemistry of DMC and, together with Platz’s analysis, of its *intramolecular* chemistry,⁷ provide a rounded portrait of the parent dialkylcarbene.

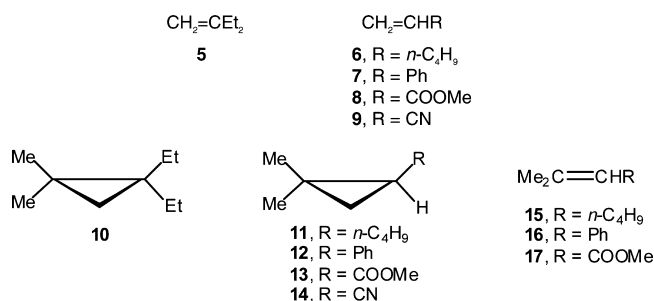
RESULTS AND DISCUSSION

Synthesis. Question 1 can be answered positively; DMC generated by the photolysis of diazirine **3** can be intercepted by a variety of olefins, albeit in yields not exceeding about 10%. Diazirine **3** was prepared by the KMnO_4 oxidation of 3,3-dimethyl-3H-diaziridine, as described by Ford et al.⁷ The diazirine was trapped in pentane at $-78 \text{ }^\circ\text{C}$ and identified by its UV spectrum: λ 345, 351, 363 nm (reported: 345, 363 nm in pentane⁸). Pentane solutions of **3** were photolyzed with alkenes **5–9** in a Rayonet photoreactor for $\sim 15 \text{ h}$ using 350 nm lamps. The corresponding cyclopropane products **10–14** were identified by GC-MS, with the parent ion (M^+) observed in each case. To buttress these assignments, cyclopropanes **11–13**

Received: December 22, 2014

Published: February 10, 2015

were independently prepared by Simmons–Smith methylenation of commercially available alkenes 15–17.



The resulting cyclopropanes were characterized by ¹H and ¹³C NMR spectroscopy and by GC-MS. Authentic cyclopropanes 11–13 were compared to 11–13 obtained from DMC additions to alkenes 6–8 by GC-MS and by GC coinjection; good agreement was found in each case.

Multiplicity. The spin multiplicity of a carbene during its reactions with an alkene is an important consideration. In the case of Ad, Platz et al. deduced from experiment that the equilibrium between the singlet and the triplet was such that, under ambient conditions in benzene, less than 0.001 of the carbene was present as the triplet.¹² This observation implied that the free energy difference between ¹Ad and ³Ad was larger than 4 kcal/mol (*T* = 298 K) in favor of ¹Ad.^{12,13} Computational studies tend to predict a marginally smaller S–T gap. For example, the gas-phase DFT computations of Parameswaran et al. (M06/def2-TZVPP//BP86/def2-TZVPP) afford $\Delta E = 3.1$ kcal/mol,¹⁴ while our CCSD(T)/cc-pVTZ//MP2/cc-pVTZ calculations predict $\Delta E = 2.7$ kcal/mol, $\Delta H = 3.2$ kcal/mol, and $\Delta G = 3.4$ kcal/mol (see Table S-4 in Supporting Information (SI) for details);¹⁵ in both cases, ¹Ad is the ground state. However, ¹Ad has a dipole moment slightly larger than that of ³Ad (computed gas-phase values are 2.7 and 1.0 D for ¹Ad and ³Ad, respectively; MP2/cc-pVTZ), and ¹Ad is hence stabilized preferentially in solution by even a nonpolar alkane solvent. Application of three different continuum dielectric solvation models predict a differential favorable stabilization of ¹Ad by 0.8–1.8 kcal/mol (*n*-pentane model solvent; see SI for details) which, when combined with the gas-phase CCSD(T)/cc-pVTZ result presented above, suggests a “best” computed estimate for the ¹Ad – ³Ad free energy difference of 4–5 kcal/mol in alkane solution, in full agreement with the suggestion advanced by Platz et al. Considering this magnitude of S–T separation and our ignorance of the rate constants for interconversion of ¹Ad and ³Ad, we interpreted the observed rate constants and philicity of the additions of Ad to alkenes 5–9 solely in terms of ¹Ad, and a coherent, consistent mechanistic analysis emerged.¹

In the present study of DMC, a similar situation is obtained. An early computational study by Schaefer et al. put the gas-phase energy difference between ¹DMC and ³DMC as $\Delta E = 1.4$ kcal/mol, with the singlet as the ground state, and concluded that both species would take part in reactions of the carbene.¹⁶ Similarly, extensive ab initio calculations on ¹DMC and ³DMC by Matzinger and Fülcher led to a best estimate for the energy difference of $\Delta E = 1.6$ kcal/mol;¹⁷ a more recent DFT study by Kassae et al. reports an energy difference of 1.2 kcal/mol (B3LYP/aug-cc-pVTZ).¹⁸ Our highest level gas-phase calculations (CCSD(T)/cc-pV6Z//CCSD/cc-pVTZ; further details in SI) provide $\Delta E = 2.2$

kcal/mol and a “best” estimate for the S–T free energy difference of $\Delta G = 1.7$ kcal/mol (*T* = 298 K), again with the singlet carbene as the ground state. Parallel to the Ad scenario above, the dipole moment of ¹DMC (2.1 D) is larger than that of ³DMC (0.7 D) and affords preferential stabilization of ca. 1.4–1.5 kcal/mol for ¹DMC in alkane solution (see Table S-5 in SI for details). A best estimate of the ¹DMC/³DMC free energy difference of ca. 3.5 kcal/mol (*T* = 298 K) results, which corresponds to a ¹DMC/³DMC distribution ratio larger than 99:1 in hydrocarbon solution. Even though the ¹DMC/³DMC free energy difference is slightly less than that for ¹Ad/³Ad we will, for simplicity, analyze the DMC chemistry that follows in terms of ¹DMC only. We will find that there is a very pronounced similarity in the behavior of both Ad and DMC.

The singlet–triplet gap computed in DMC (ca. 3.5 kcal/mol) is thus similar to that of Ad (ca. 4–5 kcal/mol), and both dialkylcarbenes are predicted to possess singlet ground states in the gas phase and in hydrocarbon solution. At the MP2/cc-pVTZ level, we find that the C–C_{carbene}–C angle attains an optimal value of 110.8° in ¹DMC and opens to 130.6° in ³DMC; both values are typical for the lowest energy singlet and triplet states of unconstrained carbenes. For Ad, however, the corresponding optimized C–C_{carbene}–C value is 111.1° in ¹Ad but only 117.8° in ³Ad; the rigid Ad skeleton impedes structural relaxation and thus preferentially disfavors the triplet state in Ad. In DMC, hyperconjugation from six optimally oriented C–H bonds stabilizes the p-orbital on the carbene center, hence preferentially favoring ¹DMC relative to ³DMC. In Ad, there are only two, nonoptimally aligned C–H bonds available for hyperconjugative interactions with the carbenic center. We conclude that the close proximity of the S–T gaps in DMC and Ad reflects a combination of factors and appears to some extent to be coincidental.

Anticipated Philicity. Table 1 displays computed HOMO/LUMO energies, absolute electrophilicities (ω),¹⁹ and stabiliza-

Table 1. Carbene Parameters

carbene	ϵ_{HO}^a	ϵ_{LU}^a	ω^b	ΔE_{stab}^c
Me ₂ C	−9.04	3.39	0.32	28.7
2-Ad	−8.39	2.96	0.33	25.8
CCl ₂	−10.91	1.00	1.03	45.5
CF ₂	−12.85	2.74	0.82	70.9
ClCOMe	−10.49	3.14	0.50	72.7
C(OMe) ₂	−10.20	4.98	0.22	92.0
MeCOMe	−9.23	4.04	0.25	59.2
C(NMe) ₂	−8.24	5.94	0.05	86.6

^a ϵ_{HO} and ϵ_{LU} are the HOMO and LUMO energies in eV, computed at the HF/6-31G(d,p)//MP2/6-31G(d,p) level, cf. refs 19a, b. ^bGlobal electrophilicity in eV; see refs 19c–e. ^cCarbene stabilization energy (ΔE_{stab}) calculated at the B3LYP/6-311++G(2d,p) level, in kcal/mol relative to CH₂. For a carbene of formula CXY, $\Delta E_{\text{stab}} = -\Delta E$ for the isodesmic reaction CH₃X + CH₃Y + CH₂ → CXY + 2CH₄, cf. ref 20.

tion energies relative to CH₂²⁰ for DMC and seven other carbenes; a more extensive table, containing additional parameters and ten more carbenes, appears in the SI as Table S-1.

We notice at once that the HOMO and LUMO energies of DMC and Ad are quite similar; the two carbenes should therefore exhibit similar philicities toward a common set of alkenes. The HOMOs of DMC and Ad are relatively high-lying

due to the absence of σ -withdrawing electronegative heteroatoms bonded to the carbene center. The orbital energies (ϵ_{HO}) of DMC and Ad resemble those of the nucleophilic carbenes MeCOMe and C(NMe₂)₂ in magnitude²¹ and are significantly higher than those of the electrophilic carbenes CCl₂ and CF₂, the ambiphilic carbene ClCOMe, and even the nucleophilic carbene C(OMe)₂; cf. Table 1. The high-lying, accessible HOMO of DMC should confer nucleophilic properties, as in the case of Ad.^{1,2}

At the same time, the electrophilicity (ω) of DMC, like that of Ad, is low compared to the electrophilic or ambiphilic carbenes of Table 1. Similarly, the LUMO energy (ϵ_{LU}) of DMC is higher than ϵ_{LU} of the electrophilic carbenes of Table 1 (CCl₂ and CF₂) or Table S-1 in SI, degrading the ability of DMC to behave as an electrophile toward alkenes. However, at 3.39 eV, ϵ_{LU} of DMC is only slightly higher than that of ambiphilic ClCOMe (3.14 eV), reminding us that DMC could potentially behave as an electrophile toward a strong nucleophile. Indeed, DMC readily reacts with the lone pair electrons of pyridine to yield ylide 4.⁷ In this, it manifests residual electrophilicity, reminding us that all carbenes are at least potentially ambiphilic.

The carbene stabilization energy, ΔE_{stab} , of DMC, like that of Ad, is much lower than those of the other carbenes in Table 1 or Table S-1 in SI. The latter are each stabilized by at least one substituent carrying lone pair electrons that can be donated to the formally vacant p orbital at the carbene centers of these singlet species. Both DMC and Ad should therefore be considerably more reactive and can be characterized as “reactive nucleophilic” carbenes. A similar description derives from Miesusset and Brinker, whose analysis of carbenic reactivity is based on computed C–H insertion energies.²² Given their reactivity toward pyridine, DMC and Ad are seen to retain residual ambiphilic potential.

We can explore the frontier molecular orbital interactions between DMC and various alkenes by deriving the differential orbital energies $\Delta E_{\text{E}} (= \epsilon_{\text{LU}}^{\text{DMC}} - \epsilon_{\text{C=C}}^{\text{HO}} = \text{p} - \pi)$ and $\Delta E_{\text{N}} (= \epsilon_{\text{C=C}}^{\text{LU}} - \epsilon_{\text{DMC}}^{\text{HO}} = \pi^* - \sigma)$, corresponding to the electrophilic and nucleophilic transition state interactions, respectively, for the reaction of DMC with an alkene.²¹ Neglecting considerations of orbital overlap, a smaller ΔE is associated with greater transition state stabilization, a lower activation energy, and a more rapid addition reaction.^{20,21} Differential orbital energies for additions of DMC to the five alkenes that we studied are collected in Tables S-2 and S-3 in SI. Irrespective of whether the alkene is electron-rich or electron-poor, $\Delta E_{\text{N}} < \Delta E_{\text{E}}$ in each case. DMC is thus predicted, like Ad,¹ to display nucleophilic selectivity toward alkenes. The philicity of DMC should resemble that of nucleophilic MeCOMe,²³ rather than that of ambiphilic ClCOMe^{21,24} or electrophilic CCl₂.^{21,25}

Kinetics. Laser flash photolysis (LFP) at 351 nm of diazirine 3 in pentane ($A_{351} = 0.5$) containing 0.154 M pyridine afforded an absorption for ylide 4 at 340 nm (see Figure S-1 in SI). No other significant transients were observed (nor by Platz et al.⁷), excluding the formation of dimethyldiazomethane. The absorption of this ylide has been reported at 390 nm in benzene¹² and at 364 nm in Freon-113.⁷ In pentane, the “yield” of the ylide, as measured by its absorbance, increased with increasing pyridine concentration between 0 and 0.153 M pyridine. Only a marginal increase in ylide absorbance was observed at a pyridine concentration of 0.184 M; see Figure 1. In measuring rate constants for DMC additions to alkenes (see

below), we used 0.154 M pyridine to “visualize” the carbene via ylide 4.

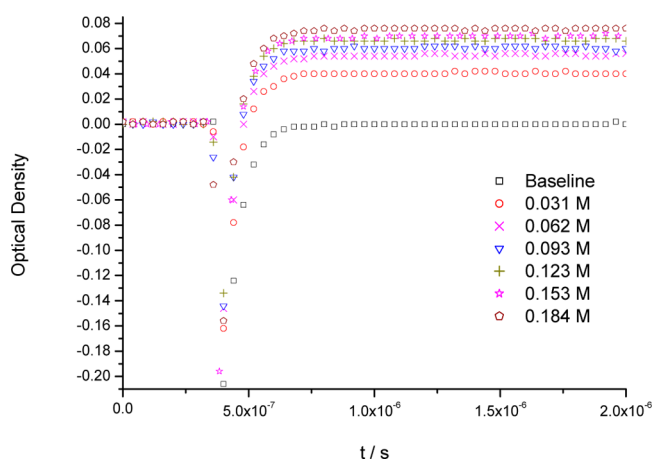


Figure 1. Absorbance of pyridinium ylide 4 at 340 nm in pentane at ambient temperature as a function of pyridine concentration; for diazirine 3, $A_{351} \sim 0.8$. The “yield” of ylide 4, formed from DMC and pyridine, increases as the concentration of pyridine increases until all of the available DMC is captured by the pyridine.

Given that diazirine 3 is irradiated with a xenon fluoride excimer laser at 351 nm, some scattered light impacts our monochromator at 340 nm, resulting in the strong “negative” absorbance visible in Figure 1 at $\sim 3 \times 10^{-7}$ s. However, at zero pyridine concentration (baseline), the photomultiplier signal returns to the same level that it exhibited before the laser emission. Moreover, analysis (using Igor Pro 6.04 software) of the optical density growth signals of ylide 4 at different pyridine concentrations produced excellent fits as single exponentials.

From Figure 3 of ref 7, we estimate Platz’s rate constant for the reaction of DMC with pyridine as $k_{\text{pyr}} \sim 1.4 \times 10^8 \text{ M}^{-1} \text{ s}^{-1}$ in Freon-113 at 5 °C. This is about 10 times slower than the reactions of, for example, the phenylhalocarbenes with pyridine.²⁶ The “electrophilic” reaction of DMC with pyridine should be influenced by the value of ϵ_{LU} , which is 3.39 eV for DMC and substantially higher than ϵ_{LU} of the phenylhalocarbenes (0.78–1.46 eV, cf. Table S-1 in SI) or the iconic electrophile CCl₂ (1.00 eV, Table 1), consistent with a slower reaction of DMC with pyridine, relative to these other carbenes.

A correlation of k_{obs} for ylide formation (from Figure 1) versus the concentration of pyridine appears in Figure 2, from which the slope gives the second-order rate constant for the reaction of DMC with pyridine as $k_{\text{pyr}} = 1.5 \times 10^7 \text{ M}^{-1} \text{ s}^{-1}$. This value is about 10 times lower than Platz’s value.⁷ Although we are unable to account for the discrepancy, it should not affect the rate constants determined for DMC additions to alkenes in which we measure the effect of added alkene on k_{obs} for ylide formation. A reviewer suggested that the discrepancy could be due to differences in solvent, temperature, or unknown experimental artifacts.

Absolute rate constants for additions of DMC to several alkenes were determined by LFP using the ylide probe method,²⁷ where the observed rate of formation of ylide 4 increases upon addition of an alkene at a constant concentration of pyridine. Linear correlation of k_{obs} for ylide formation versus [alkene] then gives a slope equal to k_{add} for the addition of DMC to the alkene.

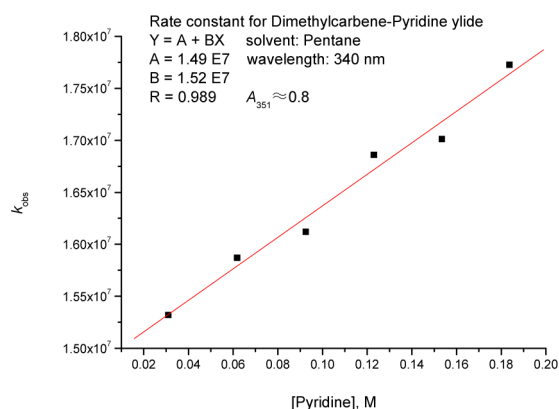


Figure 2. k_{obs} for the formation of ylide 4 versus [pyridine] (M): $k_{\text{pyr}} = 1.5 \times 10^7 \text{ M}^{-1} \text{ s}^{-1}$; $r = 0.99$.

k_{add} was measured for additions of DMC in pentane to 2-ethyl-1-butene, 1-hexene, styrene, methyl acrylate (MeAc), and acrylonitrile (AcrCN). Graphical displays of all the kinetics runs appear in SI. We selected olefin concentrations at which the ylide absorbances could be precisely measured and led to good correlations of k_{obs} and [olefin]. The ylide absorbances were fitted up to their maxima over time ranges where signal decay was minimal.

Averaged rate constants k_{add} from duplicate runs appear in Table 2, where they are compared to analogous data for Ad.^{1,2}

Table 2. Rate Constants for Additions of Dimethylcarbene to Alkenes^a

alkene	$k_{\text{DMC}} (\text{M}^{-1} \text{s}^{-1})$	$k_{\text{Ad}} (\text{M}^{-1} \text{s}^{-1})^b$
$\text{CH}_2=\text{CHCN}$	$(2.92 \pm 0.09) \times 10^7$	1.33×10^8
$\text{CH}_2=\text{CHCO}_2\text{Me}$	$(8.24 \pm 0.02) \times 10^6$	4.18×10^7
$\text{PhCH}=\text{CH}_2$	$(7.44 \pm 0.03) \times 10^5$	2.38×10^6 ^c
$\text{CH}_2=\text{CHBu}$	$(4.24 \pm 0.03) \times 10^5$	2.63×10^5
$\text{CH}_2=\text{CEt}_2$	$(3.42 \pm 0.10) \times 10^5$	1.78×10^5

^aIn pentane at 25 °C. ^bFrom ref 1. ^cFrom ref 2.

Error analysis of the original data shows that our average shot-to-shot variance is (\pm) 0.30% over 25 randomly selected runs, for all five olefins at various temperatures. Duplicate experiments (with 2 to 3 shots per point and 5 points per experiment) give k_{add} values with reproducibilities of (\pm) 3.1, 0.24, 0.40, 0.70, and 2.9% for the five olefins studied. Correlations (5 points) of k_{obs} versus [olefin] are linear with $r > 0.99$ (9 correlations), $r > 0.98$ (7 correlations), and $r > 0.97$ (2 correlations).

The rate constants measured for the additions of DMC to the five olefins are similar to those obtained for Ad.^{1,2} The HOMO and LUMO energies of DMC and Ad are similar (Table 1), so that with the same olefins, similar rate constants should be observed, dominated by the HOMO(carbene)/LUMO(alkene) nucleophilic interaction (cf. Tables S-2 and S-3 in SI).^{28,29} As predicted above, and in answer to question 2 raised in Introduction, the reactivity of DMC toward alkenes is consistent with nucleophilic selectivity and philicity, similar to that of Ad but inverse to that of the electrophilic CCl_2 .^{1,25}

Activation Parameters. Activation parameters for additions of DMC to 2-ethyl-1-butene and MeAc were derived from measurements of k_{add} at five temperatures between 274 K and 303 K, with temperatures controlled to ± 0.1 K. The individual kinetics runs and the resulting Arrhenius correlations

appear in SI. The experimentally derived activation parameters are collected in Table 3, where they are compared with corresponding data for Ad.¹

Table 3. Activation Parameters for Additions of DMC and Ad to MeAc and 2-Ethyl-1-butene^a

activation parameters	DMC		Ad	
	$\text{CH}_2=\text{CHCO}_2\text{Me}$	$\text{CH}_2=\text{CEt}_2$	$\text{CH}_2=\text{CHCO}_2\text{Me}$	$\text{CH}_2=\text{CEt}_2$
E_a	-3.5 ± 0.4	-2.0 ± 0.3	-3.6	-1.2
ΔH^\ddagger	-4.1 ± 0.4	-2.6 ± 0.3	-4.1	-1.8
ΔS^\ddagger	-40.6 ± 1.5	-42.1 ± 1.2	-38	-40
ΔG^\ddagger	8.0 ± 0.9	9.9 ± 0.7	7.1	10.3

^aErrors are derived from the Arrhenius correlations. E_a , $\Delta H^\ddagger = E_a - RT$, and ΔG^\ddagger in kcal/mol; ΔS^\ddagger in e.u. Eyring parameters are derived at $T = 298$ K.

We note the similarity between the DMC and Ad parameters, including the negative activation energies and enthalpies expected for these very reactive carbenes. We have previously encountered negative activation energies for additions to alkenes of PhCCl ,³⁰ CCl_2 ,³¹ and CF_3CCl .³² We believe that the most economical explanation for the negative Arrhenius activation energies is that offered by Houk: these carbene-alkene additions are so exothermic that the associated energy and enthalpy continually decrease along the reaction coordinate, and the activation parameters are accordingly negative.³³ Barriers to these additions occur in the free energy of activation (ΔG^\ddagger) and are generated by the very negative entropies of activation.³³

Obtaining similar results for the nucleophiles DMC and Ad shows that negative Arrhenius activation energies are a function of a carbene's reactivity, not its philicity. Computed activation energies (see below) for the additions of DMC and Ad to MeAc and 2-ethyl-1-butene are in very good agreement with the experimental values in Table 3. As with PhCCl , CCl_2 , CF_3CCl , and Ad, free energy barriers to additions of DMC to alkenes are engendered by very unfavorable entropies of activation.

Computational Studies. We have located TS's for additions of DMC to the alkene set presented in Table 2 from DFT calculations employing the MN12-SX functional³⁴ and cc-pVTZ basis sets.³⁵ Computed activation parameters are presented in Table 4 (see Table S-6 in SI for further details). The computed activation potential energies and enthalpies are negative for all five alkenes; for example, computed ΔH^\ddagger values span the narrow range from -1.4 kcal/mol (1-hexene) to -2.5 kcal/mol (styrene). For the alkenes methyl acrylate and 2-ethyl-1-butene, the computed values are $\Delta H^\ddagger = -2.3$ kcal/mol and -2.5 kcal/mol, whereas the experimental values (Table 3) are $\Delta H^\ddagger = -4.1 \pm 0.4$ kcal/mol and -2.6 ± 0.3 kcal/mol, respectively. Also, very negative entropies of activation are computed ($\Delta S^\ddagger < -30$ e.u.) for all alkene substrates; hence the presence of free energy barriers for DMC-alkene cycloaddition is clearly a reflection of highly unfavorable entropic ($-T\Delta S^\ddagger$) terms. Interestingly, the computed activation entropies appear to be less negative than the experimental ones, although they are in the range expected for a gas-phase bimolecular reaction. Specifically, for the alkenes methyl acrylate and 2-ethyl-1-butene, the computed values are $\Delta S^\ddagger = -34.1$ e.u. and -38.6 e.u., whereas the corresponding experimental values (Table 3) are $\Delta S^\ddagger = -40.6 \pm 1.5$ e.u. and -42.1 ± 1.2 e.u., respectively.

Table 4. Computed Activation Parameters for Additions of DMC to Alkenes^a

alkene	ΔE^\ddagger ^b	ΔH^\ddagger ^b	ΔS^\ddagger ^b	ΔG^\ddagger ^b	ΔG^\ddagger ^c	ΔG^\ddagger ^d	$\Delta G^\ddagger(\text{exp})$ ^e
CH ₂ =CHCN	-2.3	-1.6	-31.6	7.9	7.8	7.7	7.3
CH ₂ =CHCO ₂ Me	-3.0	-2.3	-34.1	7.9	8.0	8.8	8.0 ± 0.9
PhCH=CH ₂	-3.3	-2.5	-33.5	7.5	7.3	9.2	9.4
CH ₂ =CHBu	-2.2	-1.4	-33.5	8.6	8.6	8.6	9.6
CH ₂ =CEt ₂	-3.3	-2.5	-38.6	9.0	8.9	8.8	9.9 ± 0.7

^aEnergy values in kcal/mol, entropy values in e.u.; computed relative to the lowest energy conformers of the separated reactants. ^bMN12-SX/cc-pVTZ data. ^cObtained using CCSD(T)/cc-pVTZ values for ΔE^\ddagger and thermal corrections from the MN12-SX/cc-pVTZ calculations. ^dMN12-SX/cc-pVTZ calculations incorporating the continuum dielectric SMD model and simulated *n*-pentane solvent. ^e $\Delta G^\ddagger(\text{exp})$ derived from the Eyring equation, $k_{\text{add}} = (RT/h)\exp(-\Delta G^\ddagger/RT)$, using k_{add} data from Table 2.

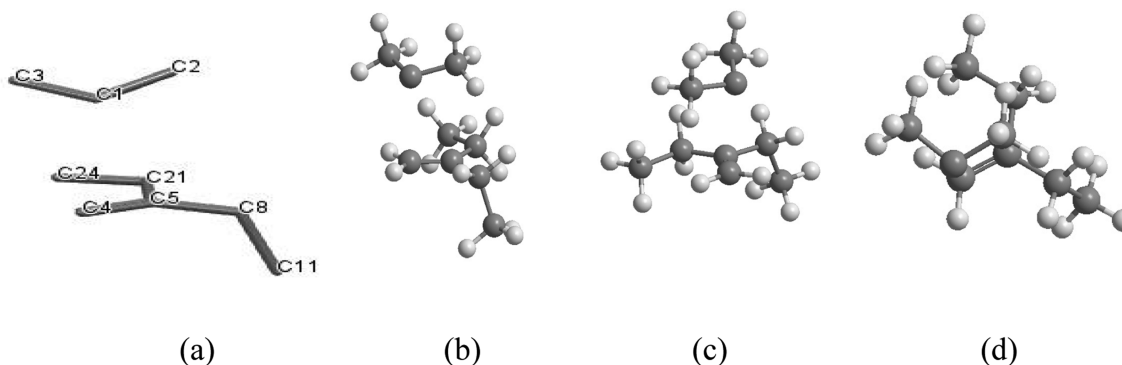


Figure 3. Transition state for DMC addition to CH₂=CEt₂. Panels: (a) Heavy-atom stick drawing and atom numbering; (b) side-on view, similar to panel a; (c) end-on view; (d) top view, showing carbene C1–C2 single bond aligned with alkene C4–C5 double bond.

The numerical agreement between experimental and computed parameters appears satisfactory.

The free energy barriers derived from the experimental measurements ($\Delta G^\ddagger(\text{exp})$, Table 4) may be roughly separated into two groups: DMC addition to CH₂=CHCN and CH₂=CHCO₂Me present the smaller barriers, whereas additions to PhCH=CH₂, CH₂=CHBu, and CH₂=CEt₂ require DMC to surmount slightly larger, but similar, barriers. The computed activation free energies, with the exception of the PhCH=CH₂ substrate, follow the observed trend; however, the overall spread in computed free energies (ca. 1.5 kcal/mol) is smaller than the experimentally derived spread (ca. 2.6 kcal/mol).

Additional single point CCSD(T)/cc-pVTZ calculations at the MN12-SX/cc-pVTZ optimized geometries change the activation energies at most by 0.2 kcal/mol (Table 4 and Table S-7 in SI). Also, reoptimization of reactant and TS structures with general solvent effects included (SMD continuum dielectric model,³⁶ *n*-pentane model solvent) changes the activation free energies by at most 2 kcal/mol relative to the idealized gas phase values (Tables 4 and Table S-8 in SI). The solvation effects from a nonpolar alkane (e.g., *n*-pentane) on the activation free energies for DMC–alkene cycloaddition appear to be very small (0.0–0.2 kcal/mol) when the alkene is CH₂=CHCN, CH₂=CHBu, or CH₂=CEt₂; larger values of approximately 0.9 and 1.7 kcal/mol are computed in the cases of CH₂=CHCO₂Me and PhCH=CH₂, respectively. Coincidentally, the relatively large solvent correction found for PhCH=CH₂ raises the computed activation energy to 9.2 kcal/mol, in fortuitously excellent agreement with the experimental value of 9.4 kcal/mol (Table 4).

Examination of the computed transition states for DMC–alkene addition reveals that they are all “early, open, and flexible,” as anticipated for reactions involving a highly reactive

species causing the appearance of negative activation energies; the TS for DMC adding to 2-ethyl-1-butene is illustrative (Figure 3). For the DMC/CH₂=CEt₂ TS, the early location of the TS on the reaction coordinate is shown by the large C1–C4 and C1–C5 distances of 2.859 and 3.167 Å, respectively. The carbene center (C1) is located above the unsubstituted alkene carbon (C1–C4–C5 = 90.6°), and the DMC plane is tilted slightly upward relative to the alkene double bond (C2–C1–C4 = 104.5°, C3–C1–C4 = 90.7°). The DMC unit has rotated relative to the conventional orientation adopted by the carbene in the TS for cycloaddition;²⁰ rather than straddling the alkene C=C bond, the C₁–C₂ single bond of DMC is aligned with the alkene double bond (C1–C2–C5–C4 = 1.0°; Figure 3, panels c and d). The structural distortions in the DMC and alkene units, relative to the free species, are minuscule: the DMC C–C bond lengths in the TS are C1–C2 = 1.477 Å and C1–C3 = 1.478 Å vs 1.469 Å in the free carbene; similarly, the C4–C5 bond length is 1.331 Å in the TS vs 1.327 Å in the free alkene. Also, the carbene angle is C2–C1–C3 = 111.4° and 111.5° in the TS and free species, respectively. The net electron transfer is only 0.03e, from DMC to CH₂=CEt₂, but in accordance with the formal classification of DMC as a nucleophile. The reaction coordinate at the TS resembles a twist mode ($\nu_{\text{imag}} = 45i \text{ cm}^{-1}$) that further orients DMC for unhindered nucleophilic attack on the alkene π -bond. It was ascertained that all the TS's located for DMC/alkene cycloaddition connect to shallow, weakly bound DMC:alkene precursor complexes in one “backward” direction along the reaction coordinate, and to the cyclopropane products in the opposite “forward” direction (procedural and energetic details available in Tables S-9 and S-10 in SI). The precursor complexes are only slightly below the TS's in energy (<1 kcal/mol) and probably do not play a role in the kinetics of cycloaddition at ambient temperature.

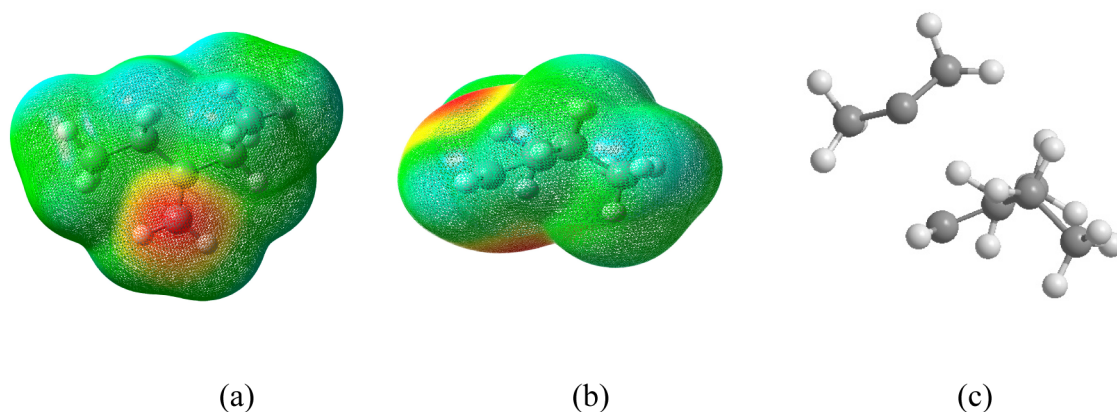


Figure 4. Molecular electrostatic potential for $\text{CH}_2=\text{C}(\text{Et})_2$. Regions in red are attractive to a negative charge. Panels: (a) Top view; (b) side-on view; (c) side-on view of precursor DMC/ $\text{CH}_2=\text{C}(\text{Et})_2$ complex.

We encountered similarly unusual orientations of the carbene in the computed structures for the precursor complexes and TS's for addition of Ad to methyl acrylate and acrylonitrile.¹ We noted that the molecular electrostatic potentials (MEPs) of these two alkenes were moderately attractive to negative charge (viz. the carbenic lone pair) in the spatial regions where Ad was located along the reaction coordinate for cycloaddition. The MEP for nonpolar 2-ethyl-1-butene (Figure 4) is similarly weakly attractive to negative charge only in the region of space above the center of the double bond where DMC is located in the cycloaddition TS (Figure 3) and precursor complex (Figure 4). Since the potential energy surface for DMC (or Ad) addition to alkenes is highly attractive in that region (cf. the negative activation energies observed and computed), it is conceivable that weak, long-range electrostatic forces might influence the approach of such highly reactive carbenes at large distances, where direct orbital overlap interactions appear to be precluded.

For completeness, we have calculated the reaction energies for the addition of DMC to the reference alkene set (cf. Table 2) in the gas phase (Table S-11 in SI) and in simulated *n*-pentane (Table S-12 in SI). Unsurprisingly, cycloaddition is highly exothermic with the computed gas-phase reaction enthalpies spanning a range from -75.6 kcal/mol ($\text{CH}_2=\text{C}(\text{Et})_2$) to -83.7 kcal/mol ($\text{CH}_2=\text{CHCN}$). For comparison, the analogous reaction enthalpies have also been computed for Ad (Table S-13 in SI); the cycloaddition reaction enthalpies for Ad are uniformly 5–7 kcal/mol more negative than those for DMC, viz. -80.7 kcal/mol ($\text{CH}_2=\text{C}(\text{Et})_2$) and -88.7 kcal/mol ($\text{CH}_2=\text{CHCN}$). The higher exothermicities computed for Ad are in qualitative accord with the remarkably low carbene stabilization energy computed for Ad (ΔE_{stab} , Table 1), which is approximately 3 kcal/mol less than that of DMC.

Conclusion. Despite a diminished intermolecular chemistry due to competitive intramolecular processes,⁷ rate constants and activation parameters can be measured for the additions of DMC to alkenes. These parameters resemble those obtained for DMC's structurally constrained analogue, adamantanylidene.¹ Both species are nucleophilic in their reactivity and selectivity toward alkenes, although vestigial electrophilicity remains, as expressed in their reactions with pyridine to form pyridinium ylides. Computational studies afford transition states and activation energies for DMC–alkene additions that are in good agreement with experiment. The activation energies are both observed and computed to be negative.

EXPERIMENTAL SECTION

General Methods. All commercially available reagents were used without further purification. Pyridine was dried over solid sodium, followed by fractional distillation. Column chromatography was performed on silica gel (200–300 mesh). ¹H NMR and ¹³C NMR spectra were recorded at 500 MHz and at 125 MHz, respectively. GC operating conditions: SPB-1 capillary column, 100 m × 0.32 mm i.d., *d*_f 1.00 μm (Supelco, Sigma-Aldrich). Flow rate of He gas, 25 mL/min. Temperatures: injector, 250 °C; detector, 300 °C; column, 60 °C (initial time, 6 min), then raised to 140 °C at 20 °C/min and retained for 10 min, then raised to 260 °C at 30 °C/min and retained for 10 min. Our LFP system is described in ref 32. Absolute rate constants for additions of DMC to several alkenes were determined by LFP using the ylide probe method,²⁷ where the observed rate of formation of ylide **4** increases upon addition of an alkene at a constant concentration of pyridine. Linear correlation of *k*_{obs} for ylide formation versus [alkene] then gives a slope equal to *k*_{add} for the addition of DMC to the alkene.

3,3-Dimethyl-3H-diazirine (3). Diazirine **3** was prepared by the KMnO_4 oxidation of 3,3-dimethyl-3H-diaziridine, as described by Ford et al.⁷ The diazirine was trapped in pentane at -78 °C and identified by its UV spectrum: λ 345, 351, 363 nm (reported: 365 nm⁷). For LFP experiments, the diazirine/pentane solution was diluted to $A_{351} \sim 0.5$. For “preparative” reactions, we used 8 mL of the diazirine/pentane solution, with $A_{351} \sim 2.5$, added to 0.4 mol of olefins **5**–**9**. These solutions were photolyzed in a Rayonet photoreactor for ~15 h using 350 nm lamps.

Cyclopropanes from DMC Additions. The cyclopropane products **10**–**14** from these photolyses were identified by GC-MS, with the parent ion (*M*⁺) observed in each case.

10: *m/e* 126 (15%) *M*⁺, 111 (13%), 96 (7%), 81 (12%), 69 (100%), 56 (61%).

GC retention time: 14.57 min.

11: *m/e* 126 (6%) *M*⁺, 111 (10%), 83 (9%), 69 (100%), 55 (83%). GC retention time 14.87 min.

12: *m/e* 146 *M*⁺ (40%), 131 (100%), 116 (13%), 103 (8%), 91 (40%), 77 (10%). GC retention time: 22.88 min.

13: *m/e* 128 *M*⁺ (46%), 113 (26%), 97 (51%), 81 (34%), 69 (92%), 55 (100%). GC retention time: 15.29 min.

14: *m/e* 95 *M*⁺ (16%), 81 (16%), 69 (100%), 56 (77%). GC retention time: 14.09 min.

Simmons–Smith Reactions. Cyclopropanes **11**–**13** were prepared by the Simmons–Smith reaction. The general synthetic method follows. Zinc–copper couple (copper content typically ca. 1–3%) was purchased from Alfa Aesar. In a 100 mL round-bottom flask containing a magnetic stirring bar, and fitted with a reflux condenser protected by a drying tube filled with Drierite, were placed three times the molar quantity to alkene of zinc–copper couple, 5 mL of anhydrous ether, and 30 mL of dichloromethane. A crystal of iodine was added, and the mixture was stirred until the purplish red color had turned to brown.

Then alkene was added and heated to gentle reflux with stirring. Three times the molar quantity to alkene of methylene iodide was slowly added (over 45 min) using a 10 mL injection syringe. The mixture was stirred under reflux for 9–24 h (olefin 17, 9 h; 16, 16 h; 15, 24 h). At the end of this time, most of the gray couple had been converted to finely divided copper. The ether solution was decanted from the copper and unreacted couple, which was then washed with two 30 mL portions of ether. The washes were combined with the decanted ether solution, and the whole was shaken with two 30 mL portions of saturated aqueous ammonium chloride solution. The ether layer was separated, dried over anhydrous magnesium sulfate, and then filtered. The filtrate was concentrated to ~5 mL and chromatographed over a short column of silica gel using 10% ether/pentane as the eluent.

1-Butyl-2,2-dimethylcyclopropane (11). This compound was isolated in 50% yield. ^1H NMR (500 MHz, CDCl_3): δ 0.01–0.03 (m, 1H), 0.50 (m, 1H), 0.55–0.65 (m, 1H), 1.05 (t, 3H), 1.17 (s, 3H), 1.18 (s, 3H), 1.34–1.56 (m, 6H); ^{13}C NMR (125 MHz, CDCl_3) δ 14.3, 15.4, 19.9, 20.1, 22.8, 25.0, 27.8, 29.7, 32.7.

1-Phenyl-2,2-dimethylcyclopropane (12).³⁷ This compound was isolated in 58% yield. ^1H NMR (500 MHz, CDCl_3): δ 0.79 (s, 3H), 0.65–0.81 (m, 2H), 1.22 (s, 3H), 1.81–1.88 (m, 1H), 7.12–7.18 (m, 3H), 7.20–7.28 (m, 2H). ^{13}C NMR (125 MHz, CDCl_3) δ 18.9, 19.4, 21.0, 28.1, 30.3, 126.0, 128.4, 129.4, 140.7.

2,2-Dimethylcyclopropane-1-carboxylate Methyl Ester (13).³⁸ This compound was isolated in 68% yield. ^1H NMR (500 MHz, CDCl_3): δ 0.70 (dd, $J = 8.1, 4.3$ Hz, 1H), 0.95–0.90 (m, 1H), 1.01 (s, 3H), 1.06 (s, 3H), 1.35 (dd, $J = 8.1, 5.5$ Hz, 1H), 3.51 (s, 3H). ^{13}C NMR (125 MHz, CDCl_3) δ 18.8, 22.1, 22.9, 26.7, 26.9, 51.3, 173.1.

■ ASSOCIATED CONTENT

● Supporting Information

Spectroscopic and kinetics data, computational details, and results. This material is available free of charge via the Internet at <http://pubs.acs.org>.

■ AUTHOR INFORMATION

Corresponding Authors

*moss@rutchem.rutgers.edu

*kroghjes@rutgers.edu

Notes

The authors declare no competing financial interest.

■ ACKNOWLEDGMENTS

We thank Professor Matthew S. Platz for several very helpful discussions. We are grateful to the National Science Foundation and to Rutgers University for financial support.

■ REFERENCES

- (1) Moss, R. A.; Wang, L.; Krogh-Jespersen, K. *J. Am. Chem. Soc.* **2014**, *136*, 4885.
- (2) Moss, R. A.; Cang, H.; Krogh-Jespersen, K. *Tetrahedron Lett.* **2014**, *55*, 4278.
- (3) Pezacki, J. P.; Warkentin, J.; Wood, P. D.; Lusztyk, J.; Yuzawa, T.; Gudmundsdottir, A. D.; Morgan, S.; Platz, M. S. *J. Photochem. Photobiol., A* **1998**, *116*, 1.
- (4) Bonneau, R.; Hellrung, B.; Liu, M. T. H.; Wirz, J. *J. Photochem. Photobiol., A* **1998**, *116*, 9.
- (5) (a) Isaev, S. D.; Yurchenko, A. G.; Murzinova, Z. N.; Stepanov, F. N.; Kolyada, G. G.; Novikov, S. S.; Karpenko, N. F. *J. Org. Chem. USSR* **1973**, *9*, 724. (b) Isaev, S. D.; Yurchenko, A. G.; Murzinova, Z. N.; Stepanov, F. N.; Kolyada, G. G.; Novikov, S. S.; Karpenko, N. F. *J. Org. Chem. USSR* **1974**, *10*, 1338.
- (6) Moss, R. A.; Chang, M. J. *Tetrahedron Lett.* **1981**, *22*, 3749.
- (7) Ford, F.; Yuzawa, T.; Platz, M. S.; Matzinger, S.; Fulscher, M. J. *Am. Chem. Soc.* **1998**, *120*, 4430.
- (8) Modarelli, D. A.; Morgan, S.; Platz, M. S. *J. Am. Chem. Soc.* **1992**, *114*, 7034.

(9) Platz, M. S. In *Advances in Carbene Chemistry*; Brinker, U. H., Ed.; JAI Press: Stamford, CT, 1998; Vol. 2, pp 133–174, esp. pp 169–170.

(10) However, a theoretical study of the photochemical decomposition of 3 was interpreted to suggest that ground-state DMC was the only source of propene: Bernardi, F.; Olivucci, M.; Robb, M. A.; Vreven, T.; Soto, J. *J. Org. Chem.* **2000**, *65*, 7847.

(11) Modarelli, D. A.; Platz, M. S. *J. Am. Chem. Soc.* **1991**, *113*, 8985.

(12) Morgan, S.; Jackson, J. E.; Platz, M. S. *J. Am. Chem. Soc.* **1991**, *113*, 2782.

(13) Bally, T.; Matzinger, S.; Truttman, L.; Platz, M. S.; Morgan, S. *Angew. Chem., Int. Ed.* **1994**, *33*, 1964.

(14) Rejisha, V. C.; Nijesh, K.; De, S.; Parameswaran, P. *Chem. Commun.* **2013**, *49*, 8465.

(15) See also Supporting Information of ref 1, p S-11.

(16) Richards, C. A., Jr.; Kim, S.-J.; Yamaguchi, Y.; Schaefer, H. F., III. *J. Am. Chem. Soc.* **1995**, *117*, 10104.

(17) Matzinger, S.; Filscher, M. P. *J. Phys. Chem.* **1995**, *99*, 10747.

(18) Kassae, M. Z.; Ghambarian, M.; Musavi, S. M.; Shakib, F. A.; Momeni, M. R. *J. Phys. Org. Chem.* **2009**, *22*, 919.

(19) (a) Moss, R. A.; Krogh-Jespersen, K. *Tetrahedron Lett.* **2013**, *54*, 4303. (b) Kiyooka, S.-i.; Kaneno, D.; Fujiyama, R. *Tetrahedron* **2013**, *69*, 4247. (c) Perez, P. *J. Phys. Chem. A* **2003**, *107*, 522. (d) Guerra, D.; Andres, J.; Chamorro, E.; Perez, P. *Theor. Chem. Acc.* **2007**, *118*, 325. (e) Parr, R. G.; Szentpaly, L. V.; Liu, S. J. *Am. Chem. Soc.* **1999**, *121*, 1922.

(20) Rondan, N. G.; Houk, K. N.; Moss, R. A. *J. Am. Chem. Soc.* **1980**, *102*, 1770.

(21) For discussions of carbenic philicity, see: (a) Moss, R. A. In *Carbene Chemistry: From Fleeting Intermediates to Powerful Reagents*; Bertrand, G., Ed.; Dekker: New York, 2002; pp 57–101. (b) Moss, R. A. *Acc. Chem. Res.* **1989**, *22*, 15. (c) Moss, R. A. *Acc. Chem. Res.* **1980**, *13*, 58.

(22) Mieusset, J.-L.; Brinker, U. H. *J. Org. Chem.* **2008**, *73*, 1553.

(23) Sheridan, R. S.; Moss, R. A.; Wilk, B. K.; Shen, S.; Wlostowski, M.; Kesselmayr, M. A.; Subramanian, R.; Kmiecik-Lawrynowicz, G.; Krogh-Jespersen, K. *J. Am. Chem. Soc.* **1988**, *110*, 7563.

(24) Moss, R. A.; Fedorynski, M.; Shieh, W.-C. *J. Am. Chem. Soc.* **1979**, *101*, 4736.

(25) Moss, R. A.; Zhang, M.; Krogh-Jespersen, K. *Org. Lett.* **2009**, *11*, 1947.

(26) Ge, C.-S.; Jang, E. G.; Jefferson, E. A.; Liu, W.; Moss, R. A.; Wlostowska, J.; Xue, S. *Chem. Commun.* **1994**, 1479.

(27) Jackson, J. E.; Soundararajan, N.; Platz, M. S.; Liu, M. T. H. *J. Am. Chem. Soc.* **1988**, *110*, 5595.

(28) There is a reasonable linear correlation ($r = 0.977$) between $\log k_{\text{DMC}}$ and $\log k_{\text{Ad}}$ for the data of Table 2, cf. Figure-S-2 in SI. The correlation's slope (0.65) suggests that DMC is somewhat less selective than Ad over this set of alkenes, presumably due to a combination of steric and electronic factors.

(29) Measurements of the rate constants for additions of Ad^{1,2} to the alkenes of Table 2 are likely to be more accurate than corresponding measurements of the DMC rate constants because the Ad-pyridinium ylide signal is much stronger, and the additions of Ad to alkenes are much more efficient⁶ than in the case of DMC. Accordingly, the proportionality of the DMC and Ad rate constants²⁸ supports the veracity of the DMC data.

(30) Moss, R. A.; Lawrynowicz, W.; Turro, N. J.; Gould, I. R.; Cha, Y. *J. Am. Chem. Soc.* **1986**, *108*, 7028.

(31) Moss, R. A.; Wang, L.; Zhang, M.; Skalit, C.; Krogh-Jespersen, K. *J. Am. Chem. Soc.* **2008**, *130*, 5634.

(32) Moss, R. A.; Wang, L.; Krogh-Jespersen, K. *J. Org. Chem.* **2013**, *78*, 11040.

(33) (a) Houk, K. N.; Rondan, N. G.; Mareda, J. *Tetrahedron* **1985**, *41*, 1555. (b) Houk, K. N.; Rondan, N. G.; Mareda, J. *J. Am. Chem. Soc.* **1984**, *106*, 4291. (c) Houk, K. N.; Rondan, N. G. *J. Am. Chem. Soc.* **1984**, *106*, 4293.

(34) Peverati, R.; Truhlar, D. G. *Phys. Chem. Chem. Phys.* **2012**, *14*, 16187.

(35) Dunning, T. H., Jr. *J. Chem. Phys.* **1989**, *90*, 1007.

(36) Marenich, A. V.; Cramer, C. J.; Truhlar, D. G. *J. Phys. Chem. B* **2009**, *113*, 6378.

(37) Prior preparations: (a) Fleming, I.; Urch, C. J. *J. Organomet. Chem.* **1985**, *285*, 173. (b) Arguello, J. E.; Penenory, A. B.; Rossi, R. A. *J. Org. Chem.* **1999**, *64*, 6115. (c) Cheng, D.; Huang, D.; Shi, Y. *Org. Biomol. Chem.* **2013**, *11*, 5588.

(38) Prior preparations: (a) McGreer, D. E.; Chiu, N. W. K. *Can. J. Chem.* **1968**, *46*, 2217. (b) Fleming, I.; Patel, S. K.; Urch, C. J. *J. Chem. Soc., Perkin Trans. 1* **1989**, 115.